International Journal of Coal Geology 310 (2025) 104886

Contents lists available at ScienceDirect

International Journal of Coal Geology

journal homepage: www.elsevier.com/locate/coal

Quantifying inertinite carbon in biochar

Hamed Sanei [a,*], Małgorzata Wojtaszek-Kalaitzidi [b], Niels Hemmingsen Schovsbo [c], Rasmus Stenshøj [a,c], Zhiheng Zhou [a], Hans-Peter Schmidt [d], Nikolas Hagemann [d], David Chiaramonti [e], Tryfonas Kiaitsis [a], Arka Rudra [a], Anna J. Lehner [f], Robert W. Brown [g,h], Sophie Gill [g], Erica Dorr [i], Stavros Kalaitzidis [j], Fariborz Goodarzi [k], Henrik Ingermann Petersen [c]

[a] Lithospheric Organic Carbon (LOC), Department of Geoscience, Aarhus University, Denmark
[b] Instytut Technologii Paliw i Energii (ITPE), Poland
[c] Geological Survey of Denmark and Greenland (GEUS), Denmark
[d] Ithaka Institute for Carbon Intelligence, Switzerland
[e] Politecnico di Torino and RE-CORD, Italy
[f] Carbonfuture GmbH, Germany
[g] Isometric, London, United Kingdom
[h] School of Environmental and Natural Science, Bangor University, Wales, United Kingdom
[i] Rainbow, Paris, France
[j] Department of Geology, University of Patras, Greece
[k] FG & Partner Ltd, Research Group, Calgary, Alberta, Canada

ARTICLE INFO

Keywords:
Biochar permanence
Inertinite benchmarking
Random reflectance (R_o)
Carbon dioxide removal (CDR)
Sampling frequency

ABSTRACT

The carbon dioxide removal (CDR) potential of biochar is determined by the long-term stability of its biogenic carbon, derived from atmospheric CO_2 fixed by photosynthesis and stabilized in solid form. This stability (carbon permanence) is commonly assessed using decay models to evaluate resistance to re-emission as greenhouse gases. However, these models are limited, as they focus primarily on short-term degradation of labile carbon fractions and are not suited to project the behavior of the highly recalcitrant component of biochar over extended timescales.

Inertinite represents highly aromatized and condensed carbon structures that are geochemically stable over millennia. This paper builds upon the Inertinite Benchmarking (*IBR$_o$2*) methodology, directly quantifying the stable carbon fraction in biochar rather than relying on modeling. The method combines thermochemical analysis and incident-light microscopy to measure the reactive (labile) component and solid carbonized macerals, respectively. Random reflectance analysis (R_o) provides a representative distribution of carbonization states, with R_o values >2.0 % defining the inertinite fraction after discounting reactive organic carbon. The R_o distribution is processed using kernel density estimation (KDE) and numerical integration to classify inertinite carbon with precision and statistical robustness.

As CDR crediting can be linked to measured inertinite content, statistical validity is essential. A Monte Carlo simulation model evaluates uncertainties from sampling frequency and production variability. Results show that increased sampling reduces uncertainty and lowers the conservative safety margin needed for potential errors. This framework supports a justified safety margin applied to reported inertinite carbon and corresponding CDR values, enabling conservative and robust crediting.

By combining direct quantification of inertinite carbon with probabilistic modeling of uncertainty, the *IBR$_o$2* method offers a transparent and rigorous framework for assessing biochar permanence, aligned with emerging international certification and national inventory methodologies.

* Corresponding author.
E-mail address: Sanei@Geo.au.dk (H. Sanei).

https://doi.org/10.1016/j.coal.2025.104886
Received 7 August 2025; Received in revised form 24 September 2025; Accepted 2 October 2025
Available online 3 October 2025

1. Introduction

The effectiveness of biochar as a means of carbon dioxide removal (CDR) depends on the permanence of its stored carbon. For soil-applied biochar, common assessment methods rely on closed-system laboratory incubations over short timeframes (often one to three years) (Budai et al., 2016; Dharmakeerthi et al., 2015; Fang et al., 2014; Herath et al., 2015; Kuzyakov et al., 2014; Major et al., 2010; Singh et al., 2012; Wu et al., 2016; Zimmerman, 2010; Zimmerman and Gao, 2013). While these experiments primarily capture the short-term decay of labile organic matter, the highly carbonized, stable fraction remains largely unreactive (Gross et al., 2024; Sanei et al., 2025). As a result, derived decay models reflect only initial degradation processes and offer no direct empirical insight into the long-term fate (> 100 years) of the stable carbon fraction, making extrapolations highly uncertain (Azzi et al., 2024; Sanei et al., 2025).

A complementary approach addresses this limitation by directly quantifying the fraction of stable carbon expected to persist over environmentally relevant timescales (>1000 years). This method draws on geological principles, recognizing that highly carbonized organic matter transforms into inertinite macerals, condensed and aromatized structures known for their resistance to degradation and long-term preservation in sedimentary rocks (Ascough et al., 2011; Ascough et al., 2010; Azzi et al., 2024; Hudspith et al., 2015; Petersen et al., 2023; Sanei et al., 2024).

Most inertinite macerals represent terminal transformation state of organic matter within the sedimentary carbon cycle, analogous with the endpoint of inorganic carbon becoming carbonate rock. From a geological perspective, inertinite macerals and carbonate minerals represent two complementary pathways of the Earth's natural long-term carbon sequestration system. Both serve as mechanisms by which atmospheric or biospheric CO_2 is transformed into rock-forming components. These transformations have over geological timescales contributed to the regulation of the Earth's climate, acting as natural thermostats during periods of elevated atmospheric CO_2. The carbonization of plant-derived organic matter into inertinite macerals, in particular, is a well-documented and geochemically validated mechanism by which the terrestrial biosphere has contributed to geological-scale carbon storage throughout Earth's history (Kroeger et al., 2011; Morga, 2011; Sanei et al., 2024; Tissot and Welte, 2013).

The Inertinite Benchmarking methodology (*IBR$_o$2*) builds on this principle by proposing direct measurement of inertinite carbon content (C_{Inert}) in biochar, which represents the portion of organic carbon that can be assumed to remain stable over millennial timescales. The recognition and quantification of the inertinite fraction within organic matter is well established in the field of organic petrology (Diessel, 1983; International Committee for Coal and Organic Petrology (ICCP), 2001; Scott and Glasspool, 2007; Morga, 2011; Petersen et al., 2023; Sanei et al., 2024; Mastalerz et al., 2023, 2025). This methodology, as applied to biochar, was described by Sanei et al. (2024) and further developed in subsequent studies (Mastalerz et al., 2025; Petersen et al., 2025; Petersen and Sanei, 2025; Rudra et al., 2024). The method was also tested in the longest-running biochar field trial in the European Union, located at La Braccesca, Italy, where Chiaramonti et al. (2024) evaluated the inertinite fraction in topsoil after 15 years. These have contributed to the refinement and streamlining of the methodology, enabling its broader application in carbon crediting frameworks and its integration into standards used by carbon registries and monitoring, reporting, and verification (MRV) systems.

While further fundamental work is needed to reconcile the maceral composition with the findings from two decades of research on carbon speciation in biochars into a coherent picture to further advance the topic of biochar persistence. However, the aim of this paper is to consolidate these developments and formally establish a standardized methodology for inertinite quantification in biochar. Building on prior research and practical application, the proposed method is presented as a best-practice approach for assessing the long-term carbon permanence of biochar in the context of CDR certification. The *IBR$_o$2* method enables certification schemes and their certification bodies to move to an advanced analysis method that allows a more nuanced and fit-for-purpose characterization of individual biochars regarding their persistence in soil.

2. Inertinite Benchmarking (*IBR$_o$2*)

The *IBR$_o$2* method integrates two complementary analytical approaches, (i) thermochemical analysis and (ii) incident light microscopy, to quantify the reactive organic carbon (C_{React}) content of biochar (Fig. 1). This is because organic matter in biochar is present in two primary forms:

(i) Reactive organic matter includes more labile compounds, consisting of secondary-generated or adsorbed material during pyrolysis such as condensates, semi-liquid tars or bituminous substances, and small carbonaceous compounds at the fringes of fused aromatic macromolecules as well as residual non-carbonized material. These are more prone to degradation but are not observable under incident light microscopy and cannot be quantified by light microscopy as introduced in the following paragraph. However, they are thermally reactive and can be volatilized through controlled re-pyrolysis. Reactive organic carbon content (C_{React}) can be quantified using thermochemical methods such as Rock-Eval 6 pyrolysis, thermal gravimetric methods, or other simmilar analysis (see Section 3).

(ii) Macerals are remaining solid and semi-solid, particulate organic matter amenable to identification and quantification using incident light microscopy (visible light), where random reflectance (R_o) can be measured. Because R_o measurements require mechanical polishing of the sample, only macerals with their solid and semi-solid nature are observable and quantifiable under the microscope (see Section 4).

To accurately determine the C_{Inert}, both carbon fractions must be quantified using separate but integrated methods ((Petersen et al., 2025; Petersen and Sanei, 2025; Sanei et al., 2024); see Section 2.3). The biochar sample is therefore divided into two representative subsamples; subsample A is subjected to thermochemical analysis to quantify the C_{React} (dry wt%), and subsample B undergoes incident-light microscopy to determine the R_o distribution of the carbonized macerals (Fig. 1).

It is critical that the sample accurately represents the entire production batch to ensure analytical accuracy and precision. Detailed guidance on appropriate sampling procedures is provided in the guidelines of the European Biochar Certificate (Schmidt et al., 2024). The use of grab samples alone can introduce high variability (Bucheli et al., 2014), which increases the risk of elevated safety margin deductions during credit issuance (see Section 5).

The procedure follows these steps (Fig. 1):

2.1. Quantify reactive organic carbon fraction

Using subsample A, the C_{React} can be measured thermochemically (see Section 3). This value, expressed as a fraction of organic carbon (C_{Org}, obtained from elemental analysis, cf. EBC 2025 (Schmidt et al., 2024) present in biochar, is defined as:

$$F_{React} = \frac{C_{React}}{C_{Org}} \quad (1)$$

Where C_{React} and C_{Org} are both expressed as weight percentages on a dry basis *(dry wt%)* and F_{React} is expressed as a fraction of reactive organic carbon (i.e., values between 0 and 1).

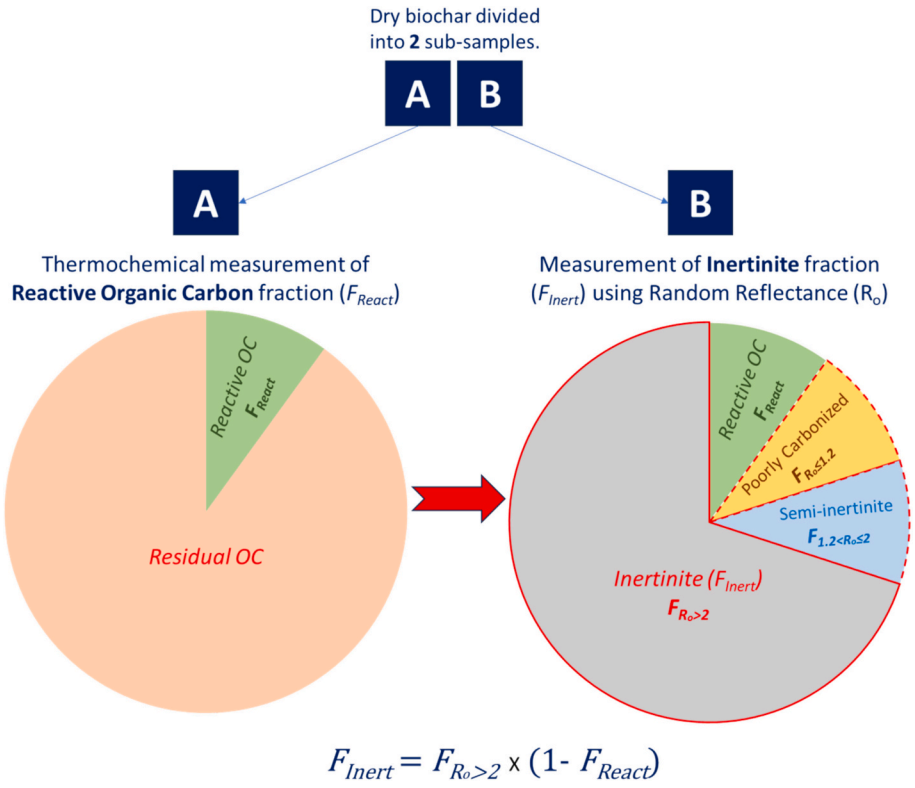

Fig. 1. Schematic protocol for quantifying the inertinite fraction of organic carbon in biochar using the inertinite benchmarking method (IBR_o2). The dry biochar sample is divided into two subsamples: (A) analyzed thermochemically to quantify the reactive organic carbon fraction (F_{React}) fraction, and (B) analyzed petrographically via reflected light microscopy to obtain random reflectance (R_o) values. Based on R_o thresholds, carbonized particles are classified as poorly carbonized ($R_o \leq 1.2$ %), semi-inertinite (1.2 % < $R_o \leq 2$ %), and inertinite ($R_o > 2$ %). The inertinite fraction of organic carbon in biochar (F_{Inert}) is calculated as the proportion of macerals with $R_o > 2$ % ($F_{Ro>2}$) multiplied by the non-reactive organic carbon fraction (1 – F_{React}).

2.2. Calculate inertinite fraction

In subsample B, reflectance can be measured at 500 points across the polished surface (see Section 3). The relative proportion of measurements with $R_o > 2.0$ % is denoted as $F_{Ro>2}$, representing the fraction of data points exceeding this threshold (Mastalerz et al., 2023, 2025; Petersen et al., 2023; Sanei et al., 2024).

$$F_{Inert} = F_{Ro>2} \times (1 - F_{React}) \quad (2)$$

Where F_{Inert} and $F_{Ro>2}$ are both expressed as fractions (i.e., nondimensional values between 0 and 1).

C_{Inert} on a dry weight basis is then calculated by, based on assumptions detailed in Section 2.3:

$$C_{Inert}\ (dry\ wt\%) = F_{Inert} \times C_{Org}(dry\ wt\%) \quad (3)$$

To quantify the CDR, the C_{Inert} is converted to its CO_2-equivalents using the molar mass ratio of CO_2/C (44.01/12.01):

$$CDR\ (wt\%) = C_{Inert}\ (dry\ wt\%) \times \frac{44.01}{12.01} \quad (4)$$

This integrated methodology provides a direct, empirical measure of the mass fraction of C_{Org} in biochar that has transformed into an inertinite-like structure. By isolating and quantifying this fraction, the IBR_o2 method offers a scientifically robust framework for assessing long-term biochar permanence in CDR applications.

2.3. Combining thermochemical and R_o methods to estimate inertinite carbon

To quantify C_{Inert} (*dry wt%*) using F_{React} and $F_{Ro>2}$ requires harmonizing differences in the units. The F_{React} is estimated as the mass ratio of carbon released during thermal decomposition, normalized to the C_{org}. In contrast, the measured $F_{Ro>2}$, derived from the volumetric distribution of R_o values, is based on the well-established point-counting method in organic petrology and represents an equally probable sampling of macerals present throughout the sample (International Organization for Standardization (ISO), 2009b; Gordon et al., 2021; Sanei et al., 2024; Zhou and Sanei, 2025). Therefore, the resulting frequency histogram of R_o values provides a statistically representative approximation of the volume fraction of biochar at different R_o classes: (i) poorly carbonized: $F_{Ro\leq1.2}$; (ii) semi-inertinite: $F_{1.2<Ro\leq2}$, and (iii) inertinite: $F_{Ro>2}$ (Sanei et al. (2024); see Section 4).

Combining the datasets reported in different units requires conversion of R_o-based volume fractions into weight percentages. Because direct measurements of maceral grain densities are not practical, the analysis assumes that all three carbonization classes (poorly carbonized, semi-inertinite, and inertinite) have identical densities. With this assumption, volume fractions are treated as equivalent to weight fractions, allowing for direct comparison without the need for density correction. In both formats, the total remains normalized to 100 %.

In reality, inertinite macerals have a higher density than other carbonaceous components due to their elevated carbon content, which results from increased aromaticity and lower volatile matter (Wang et al., 2024; Wang et al., 2023). Consequently, the common assumption of equal density across all maceral types leads to an underestimation of the inertinite contribution. For example, if the average grain densities for poorly carbonized, semi-inertinite, and inertinite components are approximately 1.30, 1.40, and 1.50 g cm^{-3} (Wang et al., 2023, 2024), respectively, and each class occupies one third of the total volume, the resulting weight distribution would be 30.9 %, 33.4 %, and 35.7 %. Thus, the actual inertinite weight fraction exceeds the estimate based on equal-density assumptions by about 2.4 percentage points. This

simplification introduces a conservative bias into the carbon accounting framework, reducing the risk of overestimating the stable carbon fraction.

3. Thermochemical measurement of reactive organic carbon

The quantification of C_{React} content in biochar can be achieved by using thermochemical analysis such as Rock-Eval 6, thermal gravimetric methods, or other similar analysis (Bordenave et al., 1993; Buss and Mašek, 2014; Lafargue et al., 1998; Petersen et al., 2023). These methods aim to re-pyrolyze the biochar sample under controlled conditions to volatilize labile carbon bonds. The mass or chemical signature of these volatile components is then used to estimate the fraction of reactive organic matter susceptible to thermal decomposition below a functionally defined temperature.

In thermal gravimetric methods, the reactive organic matter fraction (or volatime matter) is estimated gravimetrically by monitoring the sample's weight loss during pyrolysis. In contrast, Rock-Eval analysis directly measures the evolved hydrocarbons and oxygen-containing compounds using flame ionization detection (FID) and infrared (IR) spectroscopy, respectively. Since approximately 95 % of the organic molecules in biochar are composed of carbon, hydrogen, and oxygen, the sum of measured hydrocarbons, CO, and CO_2 released during pyrolysis accounts for the majority of the reactive organic matter in the biochar sample. From these evolved gases, the C_{React} content can be stoichiometrically estimated.

These methods differ in their potential biases. Rock-Eval method may underestimate C_{React}, as it does not account for minor contributions from heteroatoms such as sulfur, nitrogen, phosphorus, and trace elements. In contrast, thermal gravimetric methods may overestimate the reactive fraction, since the gravimetric signal can include weight loss from thermally unstable mineral phases, such as siderite, that decompose within the pyrolysis temperature range. Furthermore, factors such as the heating rate, maximum temperature, and residence time at the maximum temperature can also influence the measured results.

Rock-Eval 6 methodology is calibrated against Institut Français du Pétrole (IFP) standards and validated to recover the total organic carbon (C_{Org}) content. The pyrolysis stage involves heating the sample isothermally at 300 °C for 3 min, followed by a linear temperature ramp at 25 °C per minute up to 650 °C. This step facilitates the thermal degradation of labile carbon structures, releasing volatile products derived from C—H and C—O bonds. The evolved hydrocarbons, CO, and CO_2 are then quantified, and their stoichiometric carbon equivalents are used to calculate the C_{React} content, reported as a weight percentage on a dry basis (*dry wt%*) (Lafargue et al., 1998).

Following pyrolysis, the remaining sample is subjected to an oxidation phase. It is transferred to a combustion furnace, purged with air, and heated from 150 °C to 850 °C at a rate of 25 °C per minute. During this phase, the remaining organic matter is oxidized, and the resulting CO and CO_2 are measured in real time. Their stoichiometric carbon contributions define the residual organic carbon, a fraction analogous to fixed carbon (Lafargue et al., 1998; Sanei et al., 2024). The sum of reactive and residual organic carbon yields the total C_{Org} content of the biochar sample (*dry wt%*). However, the C_{Org} should still be determined by elemental analysis according to International Organization for Standardization (ISO), 2010, followed by the arithmetic deduction of inorganic carbon (Bachmann et al., 2016; Schmidt et al., 2024).

4. Random reflectance analysis of biochar

4.1. Sampling and sample preparation

The biochar sample is first dried at 40 °C, then crushed to a particle size below 0.2 mm, allowing internal cross sections of the particles to be exposed for optical measurement. After preparation, the resulting fragments are embedded in a 2.54-cm diameter cold-setting epoxy resin pellet (or similar cold-curing resin). The embedding process is carried out in two stages. In the first stage, a minimal amount of resin is mixed thoroughly with the biochar to concentrate the fragments at the base of the pellet. This is essential because biochar tends to float within the resin due to its relatively low density, and it is the base of the pellet that will later be ground and polished for microscopic analysis. Once the initial layer cures, a second layer of resin is poured to increase the pellet height for easier handling. After complete curing, the base of the pellet is ground and polished following standard procedures outlined in International Organization for Standardization (ISO) (2009a) to obtain a scratch-free, relief-free, highly polished surface. This ensures optimal exposure of biochar fragments in random orientation on the polished cross-section for reflectance measurements.

4.2. Reflectance measurement procedure

Reflectance measurements are performed using incident-, white-light microscopy. An enhanced-contrast, oil immersion 50× objective lens is recommended, and the use of a camera-based photometric system is advised due to its long-term calibration stability and precision.

The microscope should be calibrated with reflectance standards near the sample's expected R_o range, preferably using standards with higher values. A preliminary estimate of the sample's expected $R_o$can be obtained from its reported pyrolysis temperature using published empirical relationships between carbonization temperature and R_o (see Fig. 15 in Sanei et al., 2024).

Reflectance measurements should be carried out according to International Organization for Standardization (ISO), 2009b, using the smallest available light-probe diameter to minimize the effect of surface imperfections such as scratches and micro-relief, but also to avoid excluding particles with a naturally more delicate, finer structure. The size of the light probe must not exceed the area intended for measurement, in order to avoid unintentional bias from surrounding material such as scratches, debris, or adjacent phases, and to ensure that only the target surface is analyzed. Only carbonized organic matter is targeted for measurement; reflectance values are therefore inherently on an ash-free basis. Proper polishing is essential to ensure the accuracy of R_o readings and eliminate surface artefacts.

4.3. Measurement strategy and statistical requirements

Each polished pellet should be systematically examined to obtain R_o measurements from a statistically representative population of carbonized organic fragments of the biochar sample. It is recommended to collect up to three point measurements on three distinct fragments within each microscope field of view during scanning. Using the central crosshair as a guide, selections should be made from different quadrants of the field to maximize spatial randomness and avoid bias. Following the methodology outlined by Sanei et al. (2024), a total of 500 individual point measurements per sample is advised to ensure both statistical reliability and reproducibility (Fig. 2). Given a maximum of three points per frame, this corresponds to approximately 170 microscopic fields per sample. These fields should be evenly distributed across the entire polished surface to ensure representative coverage of the sample's internal heterogeneity (Fig. 2).

The mean R_o can be typically estimated with as few as 100 measurements according to International Organization for Standardization (ISO), 2009b. This estimate is based on the typical standard deviation (σ) observed in R_o datasets and a 5 % constraint on the uncertainty of the mean value. Applying the standard formula for the Standard Error of the Mean (SE), where SE represents the uncertainty in the mean estimate, the following relationship is used: $SE = 1.96\sigma/\sqrt{(N)} = 0.05$. Solving this equation provides a rough estimate of the minimum number of R_o measurements (N) required to achieve a 5 % uncertainty on the mean, assuming a normal distribution and a confidence level of approximately

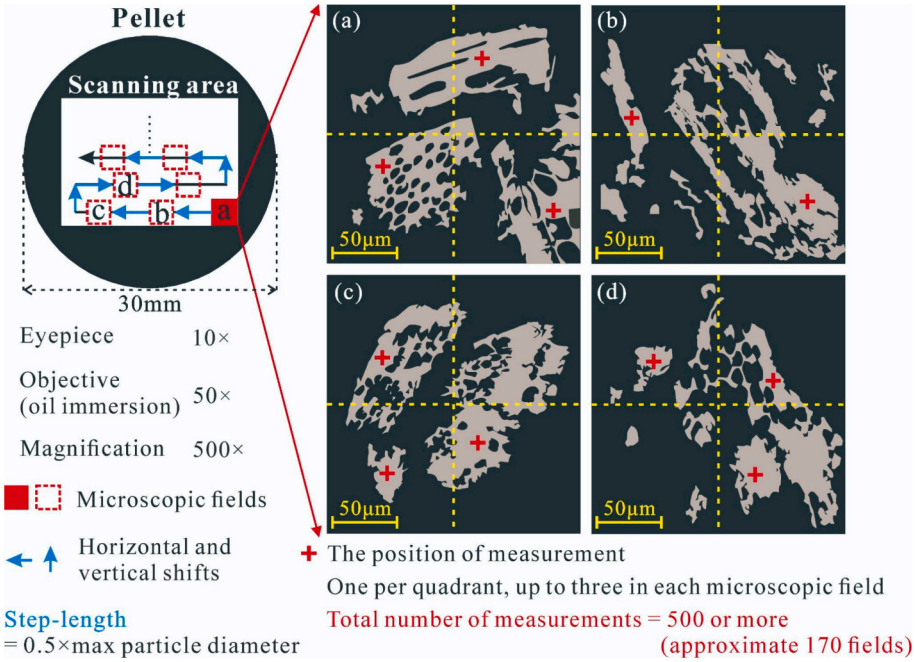

Fig. 2. Schematic illustration of the recommended protocol for measuring random reflectance (R_o) in a biochar sample. The figure shows systematic scanning of the resin-embedded pellet using a 50× oil immersion objective (total magnification 500×). Up to three R_o measurements are recommended to be taken per microscopic field of view (frames), each on a distinct maceral located in a different quadrant of the frame. Scanning continues until at least 500 individual measurements are obtained, typically requiring approximately 170 frames.

95 % (Altman and Bland, 2005; Ecampus Ontario, 2022).

However, reliable quantification of $F_{Ro>2}$ requires a representative frequency distribution of R_o values. This distribution must reflect the volumetric abundance of biochar particles across different carbonization levels and is essential for determining the fraction of highly carbonized material ($F_{Ro>2}$) (Sanei et al., 2024).

Recent work by Mastalerz et al. (2025) suggests that for low-ash, laboratory-produced lignocellulosic biochars, the number of R_o

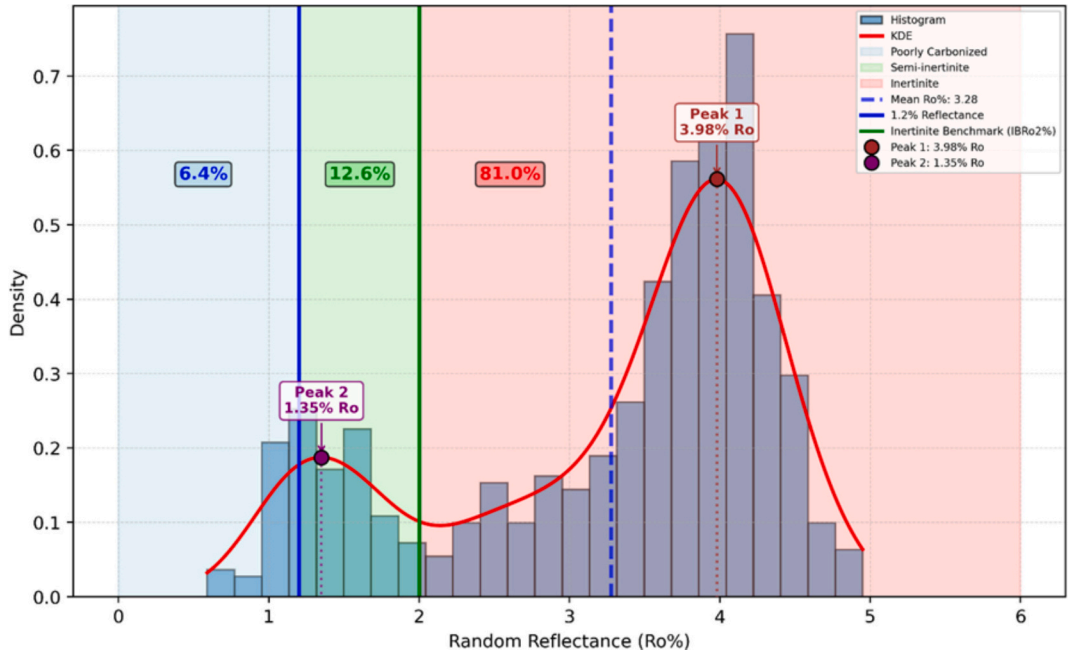

Fig. 3. Example of a bimodal distribution of random reflectance (R_o) in a biochar sample, showing the classification of carbonization stages based on R_o thresholds. The gray bars show the histogram of R_o measurements, while the red curve represents the kernel density estimate (KDE) of the R_o distribution. Color-shaded regions indicate the three carbonization classes: poorly carbonized material ($R_o \leq 1.2$ %) in light blue, semi-inertinite (1.2 % < $R_o \leq 2.0$ %) in light green, and inertinite ($R_o > 2.0$ %) in light red. The green vertical line indicates the inertinite benchmark at 2.0 % R_o (as defined in the *IBR$_o$2* method). The dashed blue line shows the mean R_o value (in this case mean $R_o = 3.28$ %). Proportions of each class are labeled within the shaded zones ($F_{Ro\leq 1.2} = 6.4$ %, $F_{1.2<Ro\leq 2} = 12.6$ %, and $F_{Ro>2} = 81.0$ %), based on the integrated area under the KDE curve. The bimodal shape reflects heterogeneous thermal conditions during pyrolysis, with a dominant mode in the inertinite range and a secondary mode in the lower reflectance region. (For interpretation of the references to color in this figure legend, the reader is referred to the web version of this article.)

measurements required to determine $F_{Ro>2}$ may in most cases be reduced to 200 without significant loss of precision. However, industrial biochars typically exhibit higher ash content and more complex, often multimodal, R_o distributions. For such materials, no consensus has yet been reached on a reduced measurement count. A global round-robin study currently underway under the auspices of the International Committee for Coal and Organic Petrology (ICCP) is expected to provide further guidance. Until more definitive evidence becomes available, the 500-point measurement protocol remains a conservative and statistically robust standard for reproducible quantification of $F_{Ro>2}$, particularly in heterogeneous industrial biochars, providing the resolution necessary for batch-level crediting and the consistency required for certification purposes (Sanei et al., 2024).

Reflectance values are plotted as frequency distributions to illustrate the spatial variability of carbonization within a biochar sample (Fig. 3). The arithmetic mean R_o provides a single value proxy for the overall degree of carbonization; however, its interpretive value depends strongly on the characteristics of the underlying distribution. In cases where the distribution is bimodal or polymodal, reflecting heterogeneous carbonization and/or heterogeneity or blending of feedstock materials, the mean R_o does not adequately represent the variability within the sample (Petersen and Sanei, 2025) (see the example in Fig. 3).

4.4. Random reflectance (R_o) profiling in biochar

The spatial distribution of carbonization levels within a biochar sample is analyzed using the frequency distribution of R_o values. The R_o data are compiled into a frequency histogram with bin widths dynamically determined to ensure statistically meaningful resolution (Fig. 3). This distribution provides a quantitative basis for assessing the extent and uniformity of carbonization, which is critical for evaluating biochar carbon stability and measuring the inertinite fraction (Sanei et al., 2024).

For instance, a critical use of the R_o distribution is the determination of the $F_{Ro>2}$ value. This can be done directly using frequency counting. However, this approach can introduce reproducibility issues in samples with complex (bi- or multimodal) R_o distributions due to inter-operator measurement variability. Operators may unintentionally select different populations of macerals and may be drawn to particles with differing reflectivity, introducing slight biases (e.g., favoring lower- or higher-reflecting particles). This leads to noticeable differences in the resulting frequency distributions and, consequently, significant differences in the calculated proportions of $F_{Ro>2}$. Such variability produces reproducibility issues for non-automated measurements that involve human operators, each with inherent differences in working style and judgment. To minimize the reproducibility impact related to R_o distribution analysis, applying kernel density estimation (KDE) is critical. KDE smooths slight inter-operator variabilities, ensuring reproducibility and reliability of fraction estimates.

4.4.1. Kernel density estimation (KDE) of R_o distribution

To obtain a continuous approximation of the distribution of R_o values, a KDE method is applied using a univariate Gaussian kernel. A Gaussian kernel is considered suitable for modeling the R_o distribution, as each component within a biochar sample is expected to follow a normal distribution when measured individually. In homogeneous samples, this yields a unimodal distribution, while heterogeneous samples produce a polymodal distribution approximated as a sum of N Gaussians, where N represents distinct components. Rather than estimating N beforehand, the KDE method captures the composite distribution directly.

KDE is a nonparametric technique that estimates the underlying probability density function $\widehat{f}(x)$ of a random variable based on a finite set of observations, without assuming any predefined distribution shape (Chen, 2017; Parzen, 1962). Given a set of measured R_o values $\{x_1, x_2, \ldots, x_n\}$, the KDE is computed as:

$$\widehat{f}(x) = \frac{1}{nh}\sum_{i=1}^{n} K\frac{(x - x_i)}{h} \tag{5}$$

Where:

- $\widehat{f}(x)$ is the estimated probability density function at point x,
- n is the number of R_o measurements (i.e., the sample size),
- x_i are the individual measured R_o values,
- h is the bandwidth, a smoothing parameter that determines the width of the kernel and controls the balance between bias and variance in the estimate,
- $K(u)$ is the Gaussian kernel function, where the variable u is defined as the standardized distance $u = \frac{x - x_i}{h}$, and $K(u)$ is given by the standard normal distribution: $K(u) = \frac{1}{\sqrt{2\pi}}\exp\left(-\frac{u^2}{2}\right)$.

The bandwidth h plays a crucial role in the shape of the resulting density estimate. A small h may lead to overfitting (a noisy estimate), while a large h may oversmooth the distribution and obscure important features. In this study, the bandwidth is selected using Silverman's rule of thumb, which provides a data-driven, closed-form solution for optimal smoothing under the assumption of normally distributed data. Silverman's rule is expressed as Silverman (2018):

$$h = 0.9\min\left(\sigma, \frac{IQR}{1.34}\right) n^{-1/5} \tag{6}$$

Where:

- σ is the standard deviation of the R_o values,
- IQR is the interquartile range of the dataset,
- n is the number of observations.

This formulation adaptively scales the bandwidth to reflect the dispersion of the data while minimizing estimation error in most practical cases.

To ensure sufficient resolution across the R_o range, the domain $x \in [x_{min}, x_{max}]$ is discretized into 500 equally spaced intervals. The resulting KDE curve is then overlaid on the empirical frequency histogram, providing a smooth and continuous representation of the R_o distribution (Fig. 3). This approach enhances visual interpretation of the carbonization profile and allows better detection of multimodality or subtle shifts in the distribution that may not be evident in the binned histogram alone.

4.4.2. Numerical integration of the KDE curve

To quantify the distribution of R_o values across different carbonization categories, the output of the KDE is numerically integrated using Simpson's rule (Talvila and Wiersma, 2012). This higher-order integration method approximates the area under the KDE curve by fitting a second-order polynomial to each pair of adjacent intervals, providing a more accurate estimate than simpler methods such as the trapezoidal rule.

$$A_{total} = \int_0^{\infty} \widehat{f}(x)dx \approx \frac{\Delta x}{3}\left[\widehat{f}(x_0) + 4\sum_{odd\ j}\widehat{f}(x_j) + 2 + \sum_{even\ j\ j\neq 0,n}\widehat{f}(x_j) + \widehat{f}(x_n)\right] \tag{7}$$

In this expression:

- A_{total} is the total area under the KDE curve, representing the integral of the estimated probability density function over the entire reflectance domain,

- $\widehat{f}(x_j)$ are the KDE-estimated density values at the discretized points x_j,
- Δx is the spacing between consecutive x-values (uniform across the interval),
- The summations are taken over odd and even indices j (excluding the endpoints for even j),
- x_0 and x_n are the lower and upper bounds of the discretized domain, respectively.

The total area is then subdivided into three carbonization categories based on R_o thresholds (Fig. 3): poorly carbonized ($R_o \leq 1.2$ %), semi-inertinite (1.2 % $< R_o \leq 2.0$ %), and inertinite ($R_o > 2.0$ %). The classification thresholds follow Sanei et al. (2024), Mastalerz et al. (2023), Mastalerz et al. (2025), Petersen and Sanei (2025), Petersen et al. (2023) and Petersen et al. (2025), with inertinite representing the most aromatized and condensed fraction, essential for long-term carbon permanence in CDR applications. Each category's partial area is calculated as:

$$A_{Ro\leq 1.2} = \int_0^{1.2} \widehat{f}(x)dx,\ \ A_{1.2<Ro<\leq 2.0} = \int_{1.2}^{2.0} \widehat{f}(x)dx, A_{Ro>2} = \int_{2.0}^{\infty} \widehat{f}(x)dx \tag{8}$$

Where $A_{Ro\leq 1.2}$, $A_{1.2<Ro\leq 2}$, and $A_{Ro>2}$ are the integrated areas corresponding to each R_o range fraction.

The relative proportions of each carbonization category are then computed by normalizing these partial areas by the total area under the KDE curve (Fig. 3):

$$F_{Ro\leq 1.2} = \frac{A_{Ro\leq 1.2}}{A_{total}}; F_{1.2<Ro\leq 2} = \frac{A_{1.2<Ro\leq 2}}{A_{total}}; F_{Ro>2} = \frac{A_{Ro>2}}{A_{total}} \tag{9}$$

Where $F_{Ro\leq 1.2}$, $F_{1.2<Ro\leq 2}$, and $F_{Ro>2}$ represent the fraction of each carbonization class.

Normalization ensures the sum of these proportions sums to 1 (100 %), accounting for rounding errors and numerical approximations inherent in the discretization and integration process.

This methodology provides a robust and reproducible framework for quantifying carbonization distributions in biochar. KDE smoothing and Simpson-rule integration enable accurate estimation of inertinite fraction within each sample. This computational workflow supports standardization and certification by enabling transparent reporting of biochar maceral composition in accordance with the *IBR$_o$2* protocol.

4.4.3. Example of biochar's R_o profiling

A case study presented here demonstrates the applicability of the KDE method through comparing two approaches for quantifying carbonization class fractions in a biochar sample with a bimodal R_o distribution (Table 1). Two operators independently measured 500 R_o points on the same polished specimen using incident light microscopy.

Table 1
Comparison of carbonization fractions in a biochar sample, independently measured by two operators using two methods: (1) direct frequency counting based on fixed R_o thresholds (Histo) and (2) kernel density estimation (KDE). Each operator analyzed 500 R_o measurements on the same polished specimen. Carbonization classes were defined as $R_o \leq 1.2$ % (poorly carbonized), 1.2 % $< R_o \leq 2.0$ % (semi-inertinite), and $R_o > 2.0$ % (inertinite). Results from direct frequency counting show higher inter-operator variability, while KDE-derived values exhibit improved agreement, demonstrating the enhanced reproducibility of KDE.

Fractions	Method	Operator 1	Operator 2	Relative Difference
$F_{Ro\leq 1.2}$	Histo:	5.6 %	6.6 %	17 %
	KDE:	5.7 %	5.6 %	1.8 %
$F_{1.2<Ro\leq 2}$	Histo:	15 %	11 %	30 %
	KDE:	13 %	12 %	10 %
$F_{Ro>2}$	Histo:	79 %	82 %	3.8 %
	KDE:	81 %	82 %	1.5 %

Carbonization classes were defined based on established reflectance thresholds: $R_o \leq 1.2$ % (poorly carbonized), 1.2% $< R_o \leq 2.0$ % (semi-inertinite), and $R_o > 2.0$ % (inertinite). The purpose was to assess how consistent the results are when derived using two different data processing methods.

The fractions were calculated using two approaches: (1) direct frequency counting, where the number of R_o points falling within each defined threshold range was counted and then normalized to the total number of measurements (500 points), and (2) kernel density estimation (KDE), in which a continuous probability density function was generated from the same dataset, and the proportion of each class was calculated by integrating the area under the KDE curve within the corresponding thresholds (Table 1).

The results show that carbonization fractions derived directly from the frequency distribution exhibit considerable variability between the two operators. This is particularly evident in the intermediate class (semi-inertinite), where relative differences between operators reached up to 30 % (Table 1). These discrepancies likely arise from the discrete nature of the dataset and the sensitivity of direct counting to small shifts in the distribution near classification boundaries. In contrast, the KDE-derived values show much closer agreement between the two operators, with relative differences consistently within <10 % for all carbonization fractions and < 1.5 % for the inertinite fraction (Table 1). This highlights the advantage of KDE in smoothing out minor local variations in the dataset, thereby reducing operator-dependent variability and enhancing reproducibility. Overall, the KDE approach provides a more reliable and consistent method for determining carbonization fractions in biochar using reflectance data.

4.5. Identification and significance of inertinite

Under incident white light, carbonized macerals in biochar are easily recognized by their gray tones (varying with reflectivity), their topographic relief compared to surrounding resin or mineral matter, and a distinctive black rim surrounding the polished surface (Petersen et al., 2023, 2025; Sanei et al., 2024). This rim is the portion of the carbonized material that remains unpolished and lies beneath the exposed cross section, still embedded within the resin matrix.

Inertinite represents a chemically inert maceral group composed of highly fused, polyaromatic carbon structures. It is characterized by high reflectivity, non-fluorescent behavior, and distinct morphological features such as vacuoles, which result from devolatilization during thermochemical conversions and from anatomical structures inherited from the original plant tissue (Diessel, 1983; International Committee for Coal and Organic Petrology (ICCP), 2001; Morga, 2011). The predominant inertinite maceral is fusinite, typically derived from lignocellulosic biomass, although other forms may originate from liptinitic matter (Hower et al., 2009).

In the context of biochar, inertinite constitutes the most chemically stable fraction of the organic matter. Reflectance measurements (R_o) exceeding 2.0 % mark the beginning of the inertinite domain in the reflectance distribution histogram (Mastalerz et al., 2025; Sanei et al., 2024). These elevated R_o values indicate extensive carbon condensation and are associated with high resistance to microbial degradation and abiotic oxidation (Petersen et al., 2025; Sanei et al., 2024). Quantifying the proportion of biochar fragments with $R_o > 2.0$ % is therefore critical for evaluating long-term carbon stability and permanence.

4.6. Inertinite R_o threshold

As discussed in the preceding sections, R_o values greater than 2.0 % have been proposed as the inertinite benchmark for biochar (Sanei et al., 2024). A common misconception is to interpret this threshold as referring to the mean R_o value. However, the $R_o > 2.0$ % benchmark denotes the lower boundary of the inertinite R_o range, not its mean (see Fig. 3). In other words, the inertinite benchmark is defined by the onset of the

reflectance distribution, not its central tendency.

This means that a sample with a mean R_o just above 2.0 % (e.g., 2.1 %) would still contain a substantial portion of reflectance values below the 2.0 % threshold. Assuming a perfectly Gaussian (normal) distribution of R_o values, nearly half of the population could fall below the inertinite threshold. Consequently, the mean R_o alone is insufficient for classifying a sample as inertinite-rich biochar.

Achieving a reflectance distribution entirely above the 2.0 % threshold under normal distribution assumptions requires a mean R_o greater than approximately 2.5 %. This distributional approach is consistent with the reflectance characteristics of inertinite-rich macerals observed in coal. Petersen et al. (2025) demonstrated that geological fusinite consistently exhibits mean R_o values exceeding 2.5 %, with structural and chemical characteristics comparable to those of highly carbonized biochars.

4.7. Advantages of reflectance over bulk chemical proxies

Unlike bulk chemical indices such as the molar *H/C* and *O/C* ratios, which can be influenced by sample heterogeneity and mineral contamination, the R_o method specifically targets carbonized organic matter in a spatially resolved manner. Because R_o values are measured directly on individual organic fragments, the results are not affected by the presence of ash or extraneous inorganic material, making the method particularly robust for high-ash biochars (Enders et al., 2012; Petersen and Sanei, 2025; Sanei et al., 2024).

In addition, reflectance analysis captures the inherent variability in carbonization across the biochar sample by providing a distribution of results rather than a bulk average, providing a spatially resolved representation of the degree of carbonization within a sample. The resulting reflectance histogram reflects the full distribution of low-, intermediate-, and highly-carbonized components, enabling a more accurate and nuanced assessment of the sample's carbonization. This is especially important for heterogeneous biochars, where carbonization may vary widely.

5. Uncertainty in inertinite quantification and its impact on CDR

This section presents a Monte Carlo simulation model developed to quantify how sampling frequency and variance in measured C_{Inert} affect the uncertainty in estimating CDR from biochar. Based on the measured variance, the model subsequently derives a statistically justified safety margin with regard to C_{Inert} quantification to be applied to reported values, ensuring conservative and reliable crediting.

In the *IBR*$_o$*2* method, the amount of CDR that can be credited is directly determined by the measured content of C_{Inert} in the biochar. However, the reported C_{Inert} value can vary due to two main sources: measurement uncertainty (from analytical variability) and sampling variability (differences between individual samples). Sampling variability is particularly important, as biochar often shows considerable heterogeneity within a single production batch (Bucheli et al., 2014), such as the annual output of a continuously operated pyrolysis facility, or between batches produced under the same conditions in discontinuously operated systems.

Preparing composite sampling, where multiple subsamples are combined into one mixed sample, can reduce the effect of small-scale variations and give a more representative sample. However, it also has a drawback in smoothing out or hiding important differences between production runs. These differences may reflect real changes in carbon stability and, if not properly accounted for, could lead to inaccurate CDR estimates.

To quantify this uncertainty, it is crucial to establish the coefficient of variation (CV) from independently collected samples of the same production batch. It is recommended to collect at least three individual samples representing either an entire batch or separate runs of a discontinuous pyrolysis unit (when assessing variability within a production process). The mean and standard deviation (σ) of C_{Inert} (*dry wt%*) from these samples are then used to calculate the CV, a key input parameter for the Monte Carlo simulation. This allows statistical uncertainty to be embedded into credit issuance rules, consistent with quality criteria set forth by frameworks such as International Organization for Standardization (ISO), 2019, the EU CRCF regulation (European Union, 2024), UNFCCC guidance (United Nations Framework Convention on Climate Change (UNFCCC), 2024), or the ICVCM assessment framework (Integrity Council for the Voluntary Carbon Market (ICVCM), 2024).

This framework makes a clear distinction between two sources of variability: (1) natural variability within a single production system or batch, including analytical and sampling uncertainty; and (2) deliberate changes made by the producer to optimize or modify the production process. The primary purpose is to assess and certify the level of variability within a defined production batch. If variability increases significantly, the framework helps determine whether this is due to random fluctuations or a modification of the production parameters. In the latter case, producers are expected to register a new batch and submit new baseline samples for analysis. Certification bodies can use the submitted data to monitor such changes. The framework allows producers to manage the homogeneity of their production and to clearly define production batches. If variability rises unexpectedly, a new batch should be started, or the system will automatically increase the safety margin applied to CDR credits. This safety margin can only be adjusted downward once additional data confirm a more consistent output.

It is also important to clarify what this method does and does not provide. The presented statistical approach does not inherently ensure the representativeness of individual samples across an extended production period or large production volumes. The model is valid when supported by adherence to representative sampling at the production premises (see Schmidt et al. (2024)). Sampling protocols must be specifically designed for the type of production, and implemented consistently using a validated procedure, whether samples are collected cross flow or from storage piles. It offers, however, a transparent, reproducible, and operator-independent means to quantify sampling-induced uncertainty at any given point in time or production interval. Producers and certification bodies should therefore interpret the resulting safety margins and CDR risk estimates as tools guiding operational decision-making and biochar carbon certification.

5.1. Variance estimation of inertinite carbon in biochar samples

Let ψ_i with $i = 1, 2, 3 \ldots$ denote the reported C_{Inert} (*dry wt%*) for i-submitted biochar samples from a production site, then the CV can be calculated using arithmetic mean ($\overline{\psi}$) and standard deviation (σ) from the sample:

$$CV = \frac{\sigma}{\overline{\psi}} = \frac{\sqrt{\left(\frac{1}{N-1}\sum_{i=1}^{N}(\psi_i - \overline{\psi})^2\right)}}{\frac{1}{N}\sum_{i=1}^{N}\psi_i} \tag{10}$$

The CV provides a normalized measure of dispersion that is independent of the magnitude of the mean and is used as a key input for risk modeling.

For a biochar production site, the total amount of inertinite carbon produced annually is estimated by multiplying the annual production (tonnes per year), by the mean C_{Inert} (*dry wt%*). The mass of inertinite carbon is then converted to its equivalent mass of removed CO_2 using the molecular mass ratio of carbon dioxide (44.01 g/mol) to elemental carbon (12.01 g/mol). This yields the baseline estimate of CDR in tonnes per year:

$$CDR_i = P_i \times \left(\frac{C_{Inert,i}^{mean}}{100}\right) \times \frac{44.01}{12.01} \tag{11}$$

Where P_i is the production volume (tonnes per year; or tonnes for a biochar batch) and $C^{mean}_{Inert,i}$ is the measured C_{Inert} (*dry wt%*). However, in practical applications, the reported mean C_{Inert} is subject to analytical and spatial variability, particularly when the sample frequency is low. To model this uncertainty, the simulation assumes that the measured C_{Inert} follows a normal distribution with a standard deviation (σ) derived from the coefficient of variation:

$$\sigma_i = \left(\frac{CV_i}{100}\right) \times C^{mean}_{inert,i} \tag{12}$$

5.2. Predicting CDR variability through Monte Carlo simulation

A Monte Carlo simulation is then used to generate synthetic sample means for different sampling frequencies. For each sampling frequency n (e.g., weekly, monthly), the model generates 1000 random sample sets. Each set consists of n individual samples drawn from the specified normal distribution. The mean of each sample set is then converted into an annual CDR estimate, yielding a distribution of 1000 possible outcomes for that sampling frequency:

$$CDR^{(n)}_j = \overline{X}^n_j \times \frac{44.01}{12.01} \times \frac{P_i}{100} \tag{13}$$

From this distribution, the model calculates the expected (mean) annual CDR and the 5th percentiles of the simulated values.

5.2.1. Quantifying CDR risk and estimating safety margins

The lower 5th percentile is interpreted as the conservative bound on creditable CDR, representing the minimum quantity of CO_2 removal that can be claimed with 95 % confidence given the sampling variability. The difference between the expected CDR and this lower bound defines the CDR risk:

$$Risk^{(n)}_{CDR} = \mu^{(n)}_{CDR} - CI^{(n)}_{5\%} \tag{14}$$

Where $\mu^{(n)}_{CDR}$ is the mean CDR value based on n independent samples, and $CI^{(n)}_{5\%}$ is the 5th percentile of the corresponding confidence interval for the same sample size.

The relative risk (%), which is also regarded as the percentage safety margin, is computed as:

$$Relative\ Risk^{(n)}_{CDR} = \left(\frac{Risk^{(n)}_{CDR}}{\mu^{(n)}_{CDR}}\right) \times 100\% \tag{15}$$

Where $Relative\ Risk^{(n)}_{CDR}$ expresses the magnitude of the risk as a percentage of the expected CDR value. This formulation allows for quantifying the safety margin by capturing the extent to which low frequency sampling increases uncertainty in reported CDR and determining the percentage that must be deducted from the reported mean to ensure conservative and statistically robust crediting.

The matrix chart shown in Fig. 4 is derived from the Monte Carlo simulation model and displays expected safety margin percentages across a range of CV values and sampling frequencies. It enables producers and certifiers to determine deduction levels appropriate to the degree of variability in measured C_{Inert} within a given production system. To apply the matrix, the CV must first be calculated from C_{Inert} values measured in at least three independent samples submitted for certification (see Sections 5 and 5.1). Once the CV is established, the matrix provides the corresponding safety margin for the intended sampling frequency (e.g., weekly, monthly, or annually).

Alternatively, when regulatory requirements do not demand exact decimal precision but only a reliable quick estimate, the reporting safety margin can be obtained from a simple closed-form formula rather than running full Monte Carlo simulations. In this formulation, the safety margin is closely reproduced by a linear relationship between CV and the inverse square root of the sampling frequency:

$$Saftey\ margin\ (\%) \approx k\ \frac{CV(\%)}{\sqrt{n}} \tag{16}$$

where n is the number of samples per year and k is a scaling constant. Across a wide range of simulations, the best fit was consistently obtained for $k \approx 1.65$, which corresponds to the one-sided 95 % confidence limit. Fig. 5a-c compare Monte Carlo simulations with the above closed-form equation using $k=1.65$, shown as dashed linear fits across three representative mean C_{Inert} values of 10, 40, and 80 wt%. With this choice of k,

Fig. 4. Matrix illustrating the reporting safety margin (%) required to account for sampling uncertainty in measured inertinite carbon content (C_{Inert}) across a range of coefficient of variation (CV) values and sampling frequencies. Sampling frequencies are expressed as number of samples per year: 96 (twice per week), 48 (weekly), 24 (biweekly), 12 (monthly), 4 (quarterly), 2 (semi-annually), and 1 (annually). Higher CV values lead to increased levels of safety margin (%) deductions from the carbon dioxide removal (CDR) credit issuance due to greater sampling variability. Conversely, increasing the number of samples per year reduces uncertainty, thereby lowering the required safety margin and improving the accuracy, credibility, and marketability of issued CDR credits for biochar facilities.

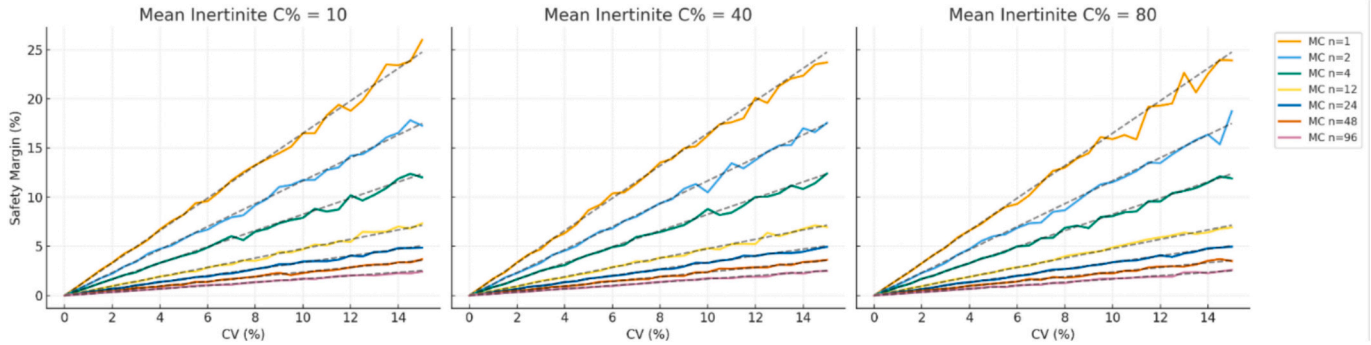

Fig. 5. Relation between the coefficient of variation (CV) of the reported inertinite carbon content (C_{Inert}) and the safety margin (%) required to account for sampling uncertainty across a range of sampling frequencies (n), expressed as number of samples per year: 96 (twice per week), 48 (weekly), 24 (biweekly), 12 (monthly), 4 (quarterly), 2 (semi-annually), and 1 (annually) (colors shown in legend). Results from the Monte Carlo simulations are compared with the simple closed-form formula: *Saftey margin* (%) $\approx k \frac{CV(\%)}{\sqrt{n}}$ with k=1.65. The equation reproduces the Monte Carlo results closely within the practical operating range of CV $\leq$ 15 %. Comparisons are shown for three representative mean C_{Inert} values of 10, 40, and 80 wt%, where dashed lines represent the closed-form expression and solid lines represent the Monte Carlo simulations.

the linear rule reproduces the Monte Carlo output with mean absolute errors below 0.2 percentage points and a maximum deviation of about 1.5–2 percentage points, even under challenging scenarios of high CV and low sampling frequency. Within the practical operating range (CV $\leq$ 15 % and mean C_{Inert} between 10 and 90 %), the closed-form expression remains robust across different distributional assumptions and closely mirrors the Monte Carlo model whether normal, lognormal, or beta noise is applied. The mean C_{Inert} has negligible influence on the relative safety margin. Because the Monte Carlo model scales the variance as a function of the mean ($\sigma \propto \mu \times$ CV), the mean cancels out when risk is expressed relative to the mean, leaving the safety margin dependent only on CV and sample size.

For applications that demand sub-percent accuracy under extreme conditions, such as very low or high C_{Inert} contents combined with high CV and minimal sampling, the full Monte Carlo approach remains preferable, as it better captures skew and boundary effects not represented by the simple linear rule. In most other cases, however, the closed-form formula with k=1.65 provides a sufficient and reliable basis for calculating safety margins.

Using either the Monte Carlo matrix or the simple closed-form approximation provides producers with a practical tool to evaluate the trade-off between the effort and cost of increased sampling and the potential credit gains achieved through reduced safety margin deductions. By adopting higher sampling frequencies and improving measurement quality, producers can retain a greater share of credited CDR while also contributing to stronger verification practices. This not only enhances confidence in individual claims but also supports the integrity of the carbon market, reducing systemic risk and benefiting producers, credit buyers, and the environment alike.

5.2.2. *A case example on sampling frequency in biochar CDR crediting*

Here a scenario-constructed case that demonstrates the impact of sampling frequency on the certainty of CDR estimates at a biochar production facility with an annual output of 1000 tons is presented (Table 2). In this example, C_{Inert} in three independent subsamples from the same production site, are 80.5, 77.2, and 83.8 (*dry wt%*). These values result in a mean of 80.5 (*dry wt%*) and a CV of 4.1 % (Table 2). This level of variability is typical for a biochar production and serves as the basis for the following risk analysis.

Our suggested Monte Carlo simulation estimates the CDR risk and the required safety margin deduction from credited removals across a range of sampling frequencies: 1 (annually), 2 (semi-annually), 4 (quarterly), 12 (monthly), 24 (biweekly), 48 (weekly), and 96 (twice per week) samples per year (Table 3).

The result shows that increasing sampling frequency reduces uncertainty in reported C_{Inert} and thereby improves the accuracy of the reported CDR (reducing CDR risk) (Fig. 6). This, in turn, justifies lower safety margin deductions from credited CO_2 removals (Fig. 7). The relationship between sampling frequency and the safety margin is inverse and nonlinear (Fig. 7). As sampling frequency increases, the distribution of possible mean values becomes narrower, reducing both the absolute and relative difference between the expected mean and the 5th percentile. With reference to the same feedstock and pyrolysis process, at low sampling frequencies (e.g., one or two samples per year), the uncertainty in the reported mean is higher, and hence the resulting safety margin that must be applied to ensure conservative crediting is correspondingly larger. This can lead to a significant undercrediting of the actual CDR potential, penalizing producers for low frequency

Table 2
Statistical summary of inertinite carbon content (C_{Inert}) based on three replicate values from spatially and temporally distinct subsamples of biochar produced at a facility with an annual production of 1000 tons.

C_{Inert} for Sample 1	80.5 (dry wt%)
C_{Inert} for Sample 2	77.2 (dry wt%)
C_{Inert} for Sample 3	83.8 (dry wt%)
n (number of measurements):	***3***
Mean C_{Inert}:	***80.5 (dry wt%)***
Standard Deviation (σ):	***3.3 (dry wt%)***
Standard Error (SE):	***1.9 (dry wt%)***
Coefficient of Variation (CV):	***4.1 %***

Table 3
Results of a Monte Carlo simulation showing the effect of sampling frequency on the estimated carbon dioxide removal (CDR) for a case scenario of a biochar facility with an annual production of 1000 tons, mean *inertinite carbon* (C_{Inert}) of 80.5 (*dry wt%; n = 3*) and a coefficient of variation (CV) of 4.1 % (Table 2). The table summarizes the mean CDR, the lower bound at the 5th percentile, the expected CDR risk (difference between mean and 5th percentile), and the recommended reporting safety margin for each sampling frequency.

Samples per year	Frequency	Mean CDR (t yr^{-1})	Lower Bound 5th percentile (t yr^{-1})	CDR Risk Mean-5th percentile (t yr^{-1})	Safety Margin (%)
1	Annually	2960	2764	196	6.6
2	Semi-annually	2951	2815	136	4.6
4	Quarterly	2953	2849	104	3.5
12	Monthly	2952	2895	57	1.9
24	Biweekly	2952	2914	38	1.3
48	Weekly	2952	2923	30	1.0
96	Twice a week	2952	2932	20	0.7

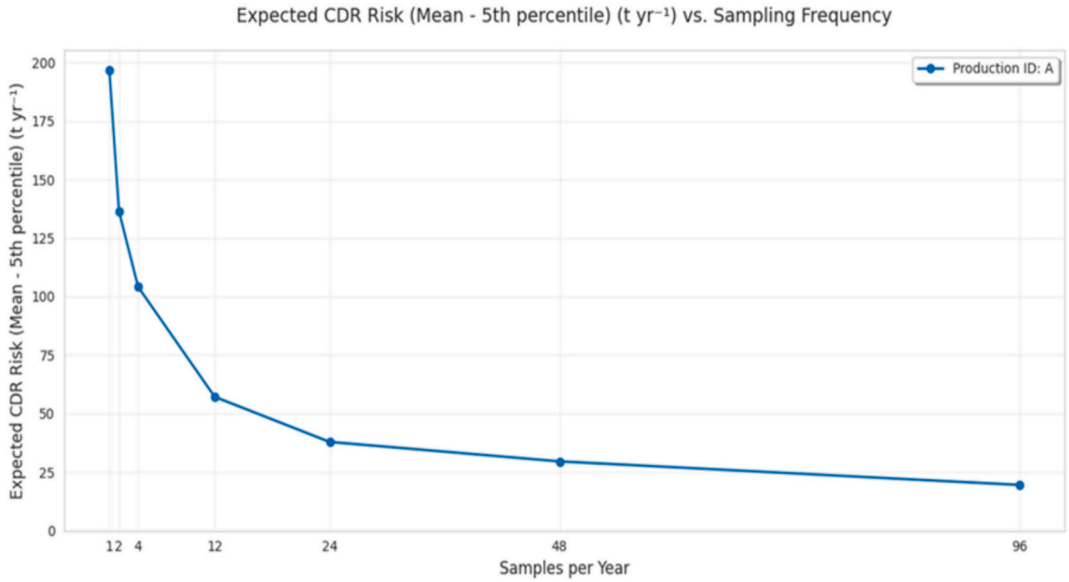

Fig. 6. Effect of sampling frequency on carbon dioxide removal (CDR) risk for a case scenario of biochar facility with 1000 tons annual output, a mean *inertinite carbon* (C_{Inert}) of 80.5 (*dry wt%* for three subsamples) with a coefficient of variation (CV) of 4.1 % (Table 2). CDR risk is defined as the difference between the mean and 5th percentile CDR from Monte Carlo simulation. Increased sampling frequency significantly reduces uncertainty in reported CDR values.

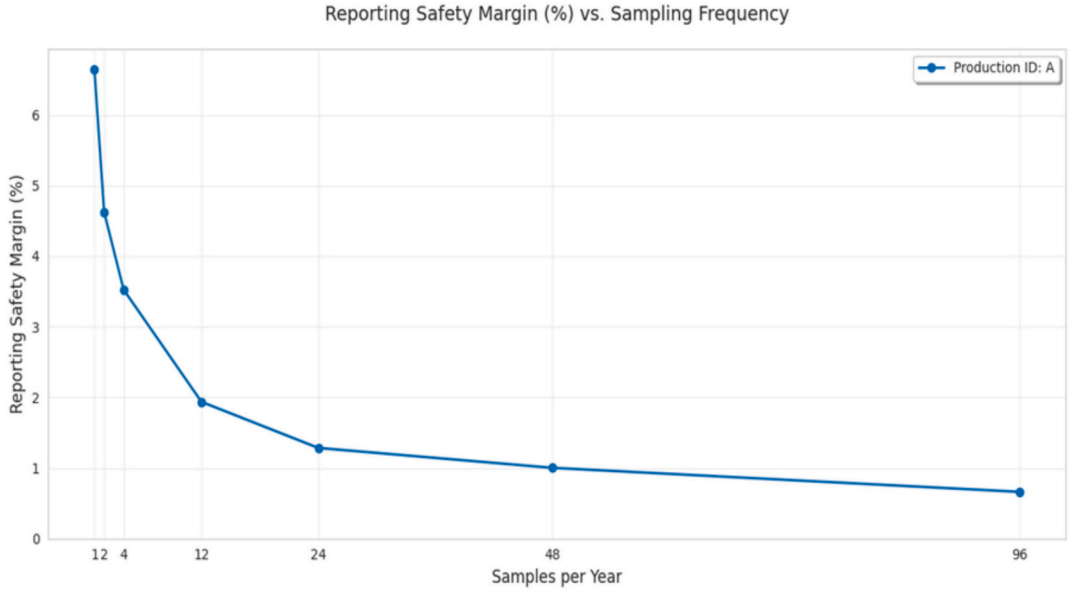

Fig. 7. Recommended reporting safety margin as a function of sampling frequency for a case scenario of biochar facility with 1000 tons annual output, reported inertinite carbon (C_{Inert}) of mean 80.5 (*dry wt%* for three subsamples) with a coefficient of variation (CV) of 4.1 % (Table 2). The safety margin is expressed as a percentage of mean carbon dioxide removal (CDR), based on expected risk from Monte Carlo simulation. Increased sampling frequency reduces uncertainty and allows for more precise CDR reporting, thereby requiring a smaller safety margin deduction from the reported CDR.

sampling.

Conversely, as the frequency of samples increases, the standard error of the mean decreases, which leads to a progressive narrowing of the confidence interval and a reduced need to apply large deductions to reported CDR values. At sufficiently high sampling frequencies, the reduction in CDR risk begins to plateau, indicating diminishing returns on additional sampling (Fig. 6). This trade-off between sampling effort and conservative margin can be visualized as a curve where the safety margin asymptotically approaches a lower bound (Fig. 7).

In this case, monthly sampling (12 samples per year) offers an optimal balance between statistical confidence and operational feasibility. It substantially reduces both CDR risk and the required safety margin without incurring excessive sampling (Table 3, Figs. 6–7).

Fig. 8 further highlights how increased sampling frequency reduces the risk of over-crediting and the size of the safety margin deduction. As sampling moves from annual to monthly or more frequently, the uncertainty in estimated CDR decreases substantially. For example, increasing the frequency from annual (1 sample/year) to monthly (12 samples/year) reduces the safety margin deduction from over 6.6 % to less than 2 %.

This tradeoff allows biochar producers to select a sampling strategy that reflects their operational capacity and budget, while maximizing credit yield and ensuring transparency. Although higher sampling frequency entails additional cost, it enhances credit integrity and market

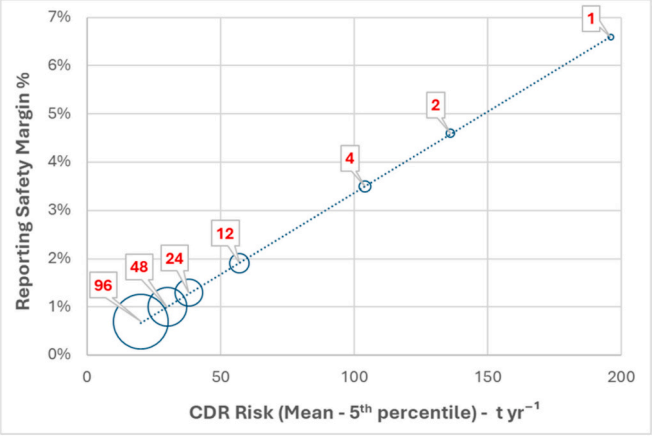

Fig. 8. Relationship between sampling frequency and carbon dioxide removal (CDR) risk, with implications for safety margin deductions in a case scenario of a biochar facility with 1000 tons annual output, mean *inertinite carbon* (C_{Inert}) of 80.5 (*dry wt%; n = 3*) with a coefficient of variation (CV) of 4.1 % (Table 2). The x-axis represents CDR risk, defined as the difference between the mean and 5th percentile of the estimated CDR distribution (t yr^{-1}). The y-axis shows the reporting safety margin (%), representing credit issuance deductions applied to account for uncertainty. Bubble sizes indicate sampling frequency per year: 96 (twice per week), 48 (weekly), 24 (biweekly), 12 (monthly), 4 (quarterly), 2 (semi-annually), and 1 (annually). Higher sampling frequencies reduce uncertainty and reporting deductions, improving the accuracy and marketability of issued carbon credits.

confidence, ultimately leading to greater financial and environmental returns.

The simulation results show the importance of sampling frequency in determining the reliability of reported values. Producers who implement frequent sampling and maintain low CV could be subject to minimal deductions. In contrast, those with sparse sampling must apply more conservative safety margins, which diminish the amount of reportable CDR credits. This framework ensures conservative and statistically robust crediting, while also incentivizing producers to adopt more rigorous and consistent production monitoring and sampling practices.

6. Conclusions

This study presents a standardized method to quantify the stable carbon fraction in biochar without relying on projected decay models. The approach, known as inertinite benchmarking (*IBR_o2*), directly measures the inertinite carbon fraction by combining incident light microscopy with thermochemical analysis. Inertinite is defined as the portion of organic matter with random reflectance (R_o) values greater than 2.0 %, corrected for the reactive organic carbon, and reported as inertinite carbon content (C_{Inert} *dry wt%*).

Since C_{Inert} is used as the basis for crediting permanent carbon storage, ensuring accuracy and reproducibility of measurements is essential. This study introduces a kernel density estimation (KDE) method to process R_o distributions, minimizing inter-operator variability. Results show that the KDE procedure yields consistent inertinite measurements across different operators, which enhances inter-laboratory reproducibility.

In addition to analytical reproducibility, the method addresses variability between samples. Since accounting of CDR is calculated from C_{Inert}, it is important to characterize the uncertainty associated with sample-to-sample variation. This requires measuring C_{Inert} in at least three independently collected samples. A Monte Carlo simulation is used to assess how this variability affects creditable removals and to define a conservative safety margin that could be subtracted from the reported mean to ensure reliable crediting.

The simulation results confirm that the required safety margin is highest when only a few samples are analyzed and decreases as sampling frequency increases. Sampling uncertainty becomes especially significant at large production volumes, where variation can greatly amplify its impact on credit estimates. The simulation framework allows producers and verification bodies to determine appropriate safety margins based on production consistency and number of samples analyzed.

CRediT authorship contribution statement

Hamed Sanei: Writing – review & editing, Writing – original draft, Visualization, Validation, Supervision, Software, Resources, Project administration, Methodology, Investigation, Funding acquisition, Formal analysis, Data curation, Conceptualization. **Małgorzata Wojtaszek-Kalaitzidi:** Writing – review & editing, Methodology, Investigation, Formal analysis. **Niels Hemmingsen Schovsbo:** Writing – review & editing, Writing – original draft, Validation, Investigation, Conceptualization. **Rasmus Stenshøj:** Writing – review & editing, Validation, Investigation. **Zhiheng Zhou:** Writing – review & editing, Validation, Methodology. **Hans-Peter Schmidt:** Writing – review & editing, Validation, Methodology, Investigation, Conceptualization. **Nikolas Hagemann:** Writing – review & editing, Validation, Methodology, Investigation. **David Chiaramonti:** Writing – review & editing, Validation, Investigation, Conceptualization. **Tryfonas Kiaitsis:** Validation, Software, Investigation, Formal analysis, Conceptualization. **Arka Rudra:** Methodology. **Anna J. Lehner:** Writing – review & editing, Validation, Methodology, Investigation. **Robert W. Brown:** Writing – review & editing, Validation, Investigation. **Sophie Gill:** Writing – review & editing, Investigation. **Erica Dorr:** Writing – review & editing, Investigation. **Stavros Kalaitzidis:** Writing – review & editing, Investigation. **Fariborz Goodarzi:** Writing – review & editing, Investigation. **Henrik Ingermann Petersen:** Writing – review & editing, Writing – original draft, Visualization, Validation, Project administration, Methodology, Investigation, Funding acquisition, Formal analysis, Conceptualization.

Author statement

I, the undersigned corresponding author, on behalf of all co-authors, confirm that the manuscript titled "**Quantifying Inertinite Carbon in Biochar**" is our original work and has not been published or submitted elsewhere for publication. All authors have made substantial contributions to the research, analysis, and manuscript preparation, and have reviewed and approved the final version for submission.

We further confirm that this manuscript has been prepared in accordance with the ethical guidelines of the journal. All data and interpretations are our own and properly cited where applicable.

Declaration of competing interest

The lead author and some co-authors have professional affiliations or collaborative relationships with organizations active in the field of biochar carbon dioxide removal, including Fusinite Ltd., United Kingdom (carbon storage security analytics and certification); the Ithaka Institute for Carbon Intelligence, Switzerland (biochar research, development of C-sink certification standards for Carbon Standards International AG, and policy consulting); Carbonfuture GmbH, Germany (digital monitoring, reporting, and verification provider and CDR trader); Isometric, United Kingdom, and Rainbow, France (Carbon standard and certification platforms); RE-CORD, Italy (no-profit public-private research center on biomass thermochemical and biochemical conversion technologies); and Biochar Europe (a pan-European network connecting science, policy, and industry in biochar). These affiliations have not influenced the design, execution, or conclusions of this study.

Acknowledgements

This study was conducted as part of a project funded by the Danish Ministry of Climate, Energy and Utilities (Klima-, Energi- og Forsyningsministeriet), as well as the INNO-CCUS project BIOCHSTA, funded by Innovation Fund Denmark and the European Union NextGenerationEU. Ithaka Institut gGmbH was financially supported within the EU Horizon Europe Project 101083780—NET-Fuels.

Data availability

Data will be made available on request.

References

Altman, D.G., Bland, J.M., 2005. Standard deviations and standard errors. BMJ 331, 903.
Ascough, P.L., Bird, M.I., Scott, A.C., Collinson, M.E., Cohen-Ofri, I., Snape, C.E., Le Manquais, K., 2010. Charcoal reflectance measurements: implications for structural characterization and assessment of diagenetic alteration. J. Archaeol. Sci. 37, 1590–1599.
Ascough, P., Bird, M., Francis, S., Thornton, B., Midwood, A., Scott, A., Apperley, D., 2011. Variability in oxidative degradation of charcoal: influence of production conditions and environmental exposure. Geochim. Cosmochim. Acta 75, 2361–2378.
Azzi, E.S., Li, H., Cederlund, H., Karltun, E., Sundberg, C., 2024. Modelling biochar long-term carbon storage in soil with harmonized analysis of decomposition data. Geoderma 441, 116761.
Bachmann, H.J.R., Bucheli, T.D., Dieguez-Alonso, A., Fabbri, D., Knicker, H., Schmidt, H.-P., Ulbricht, A., Becker, R., Buscaroli, A., Buerge, D., 2016. Toward the standardization of biochar analysis: the COST action TD1107 interlaboratory comparison. J. Agric. Food Chem. 64, 513–527.
Bordenave, M., Espitalié, J., Leplat, P., Oudin, J., Vandenbroucke, M., 1993. Screening techniques for source rock evaluation. Appl. Pet. Geochem. 217–278.
Bucheli, T.D., Bachmann, H.J., Blum, F., Bürge, D., Giger, R., Hilber, I., Keita, J., Leifeld, J., Schmidt, H.-P., 2014. On the heterogeneity of biochar and consequences for its representative sampling. J. Anal. Appl. Pyrolysis 107, 25–30.
Budai, A., Rasse, D.P., Lagomarsino, A., Lerch, T.Z., Paruch, L., 2016. Biochar persistence, priming and microbial responses to pyrolysis temperature series. Biol. Fertil. Soils 52, 749–761.
Buss, W., Mašek, O., 2014. Mobile organic compounds in biochar–a potential source of contamination–phytotoxic effects on cress seed (*Lepidium sativum*) germination. J. Environ. Manag. 137, 111–119.
Chen, Y.-C., 2017. A tutorial on kernel density estimation and recent advances. Biostat. Epidemiol. 1, 161–187.
Chiaramonti, D., Lotti, G., Vaccari, F.P., Sanei, H., 2024. Assessment of long-lived Carbon permanence in agricultural soil: Unearthing 15 years-old biochar from long-term field experiment in vineyard. Biomass Bioenergy 191, 107484.
Dharmakeerthi, R.S., Hanley, K., Whitman, T., Woolf, D., Lehmann, J., 2015. Organic carbon dynamics in soils with pyrogenic organic matter that received plant residue additions over seven years. Soil Biol. Biochem. 88, 268–274.
Diessel, C.F., 1983. Carbonization reactions of inertinite macerals in Australian coals. Fuel 62, 883–892.
Ecampus Ontario, 2022. Calculating the Sample Size for a Confidence Interval, Introduction to Statistics. Ecampus Ontario Press.
Enders, A., Hanley, K., Whitman, T., Joseph, S., Lehmann, J., 2012. Characterization of biochars to evaluate recalcitrance and agronomic performance. Bioresour. Technol. 114, 644–653.
Fang, Y., Singh, B.P., Singh, B., 2014. Temperature sensitivity of biochar and native carbon mineralisation in biochar-amended soils. Agric. Ecosyst. Environ. 191, 158–167.
Gordon, J.B., Sanei, H., Ardakani, O.H., Pedersen, P.K., 2021. Effect of sediment source on source rock hydrocarbon potential; an example from the Kimmeridgian and Tithonian-aged source rocks of the central ridge, off-shore Newfoundland, Canada. Mar. Pet. Geol. 127, 104965.
Gross, A., Bromm, T., Polifka, S., Fischer, D., Glaser, B., 2024. Long-term biochar and soil organic carbon stability–evidence from field experiments in Germany. Sci. Total Environ. 954, 176340.
Herath, H., Camps-Arbestain, M., Hedley, M., Kirschbaum, M., Wang, T., Van Hale, R., 2015. Experimental evidence for sequestering C with biochar by avoidance of CO 2 emissions from original feedstock and protection of native soil organic matter. GCB Bioenergy 7, 512–526.
Hower, J.C., O'Keefe, J.M., Watt, M.A., Pratt, T.J., Eble, C.F., Stucker, J., Richardson, A. R., Kostova, I.J., 2009. Notes on the origin of inertinite macerals in coals: observations on the importance of fungi in the origin of macrinite. Int. J. Coal Geol. 80, 135–143.
Hudspith, V.A., Belcher, C.M., Kelly, R., Hu, F.S., 2015. Charcoal reflectance reveals early Holocene boreal deciduous forests burned at high intensities. PLoS One 10, e0120835.
Integrity Council for the Voluntary Carbon Market (ICVCM), 2024. Core Carbon Principles Assessment Framework – 4: Methodological requirements (Version 1.1), London, United Kingdom.
International Committee for Coal and Organic Petrology (ICCP), 2001. The new inertinite classification (ICCP System 1994). Fuel 80, 459–471.
International Organization for Standardization (ISO), 2009a. ISO 7404-2, 2009 (E): Methods for the Petrographic Analysis of Coals — Part 2: Methods of Preparing Coal Samples, Switzerland.
International Organization for Standardization (ISO), 2009b. ISO 7404-5, 2009: Methods for the Petrographic Analysis of Coals — Part 5: Method of Determining Microscopically the Reflectance of Vitrinite, Switzerland.
International Organization for Standardization (ISO), 2010. ISO 29541:2010: Solid Mineral Fuels — Determination of Total Carbon, Hydrogen and Nitrogen — Instrumental Method. International Organization for Standardization, Geneva, Switzerland.
International Organization for Standardization (ISO), 2019. ISO 14064-2, 2019: Greenhouse Gases — Part 2: Specification with Guidance at the Project Level for Quantification, Monitoring and Reporting of Greenhouse Gas Emission Reductions or Removal Enhancements, Geneva.
Kroeger, K., di Primio, R., Horsfield, B., 2011. Atmospheric methane from organic carbon mobilization in sedimentary basins—the sleeping giant? Earth Sci. Rev. 107, 423–442.
Kuzyakov, Y., Bogomolova, I., Glaser, B., 2014. Biochar stability in soil: decomposition during eight years and transformation as assessed by compound-specific 14C analysis. Soil Biol. Biochem. 70, 229–236.
Lafargue, E., Marquis, F., Pillot, D., 1998. Rock-Eval 6 applications in hydrocarbon exploration, production, and soil contamination studies. Rev. Inst. Fr. Pét. 53, 421–437.
Major, J., Lehmann, J., Rondon, M., Goodale, C., 2010. Fate of soil-applied black carbon: downward migration, leaching and soil respiration. Glob. Chang. Biol. 16, 1366–1379.
Mastalerz, M., Drobniak, A., Briggs, D., Bradburn, J., 2023. Variations in microscopic properties of biomass char: Implications for biochar characterization. Int. J. Coal Geol. 271, 104235.
Mastalerz, M., Drobniak, A., Liu, B., Sauer, P.E., 2025. Reflectance as an indicator of biochar permanence. Int. J. Coal Geol. 306, 104809.
Morga, R., 2011. Reactivity of semifusinite and fusinite in the view of micro-Raman spectroscopy examination. Int. J. Coal Geol. 88, 194–203.
Parzen, E., 1962. On estimation of a probability density function and mode. Ann. Math. Stat. 33, 1065–1076.
Petersen, H.I., Sanei, H., 2025. The H/C Molar Ratio and its potential pitfalls for determining Biochar's Permanence. GCB Bioenergy 17, e70049.
Petersen, H.I., Lassen, L., Rudra, A., Nguyen, L., Do, P., Sanei, H., 2023. Carbon stability and morphotype composition of biochars from feedstocks in the Mekong Delta, Vietnam. Int. J. Coal Geol. 271, 104233.
Petersen, H., Stokes, M., Hackley, P., Rudra, A., Zhou, Z., Sanei, H., 2025. micro-Raman indicates biochar has similar stability and structural features as natural fusinite and semifusinite. Int. J. Coal Geol. 304, 104769.
Rudra, A., Petersen, H.I., Sanei, H., 2024. Molecular characterization of biochar and the relation to carbon permanence. Int. J. Coal Geol. 291, 104565.
Regulation (EU) 2024/3012 of the European Parliament and of the Council of 27 November 2024 establishing a Union certification framework for permanent carbon removals, carbon farming and carbon storage in products, OJ L 6.12.2024, pp. 1-29.
Sanei, H., Rudra, A., Przyswitt, Z.M.M., Kousted, S., Sindlev, M.B., Zheng, X., Nielsen, S. B., Petersen, H.I., 2024. Assessing biochar's permanence: an inertinite benchmark. Int. J. Coal Geol. 281, 104409.
Sanei, H., Petersen, H.I., Chiaramonti, D., Masek, O., 2025. Evaluating the two-pool decay model for biochar carbon permanence. Biochar 7, 9.
Schmidt, H.P., Bucheli, T., Kammann, C., Glaser, B., Abiven, S., Leifeld, J., Soja, G., Hagemann, N., 2024. European Biochar Certificate - Guidelines for a Sustainable Production of Biochar. EBC, Frick, Switzerland.
Scott, A.C., Glasspool, I.J., 2007. Observations and experiments on the origin and formation of inertinite group macerals. Int. J. Coal Geol. 70, 53–66.
Silverman, B.W., 2018. Density Estimation for Statistics and Data Analysis. Routledge.
Singh, B.P., Cowie, A.L., Smernik, R.J., 2012. Biochar carbon stability in a clayey soil as a function of feedstock and pyrolysis temperature. Environ. Sci. Technol. 46, 11770–11778.
Talvila, E., Wiersma, M., 2012. Simple derivation of basic quadrature formulas. arXiv preprint arXiv:1202.0249.
Tissot, B.P., Welte, D.H., 2013. Petroleum Formation and Occurrence. Springer Science & Business Media.
United Nations Framework Convention on Climate Change (UNFCCC), 2024. Guidance on methodologies for monitoring, reporting and quantification of removals. In: Document A6.4-SBM/2024/014/A06, Bonn, Germany.
Wang, X., Wang, S., Zhao, Y., Liu, Y., 2023. Construction and verification of vitrinite-rich and inertinite-rich Zhundong coal models at the aggregate level: new insights from the spatial arrangement and thermal behavior perspective. RSC Adv. 13, 7569–7584.
Wang, A., Zhao, M., Li, X., Cao, D., Wei, Y., Wang, L., 2024. Pressure effects on molecular evolution: differences between vitrinite and inertinite in coal. Fuel Process. Technol. 256, 108066.
Wu, M., Han, X., Zhong, T., Yuan, M., Wu, W., 2016. Soil organic carbon content affects the stability of biochar in paddy soil. Agric. Ecosyst. Environ. 223, 59–66.
Zhou, Z., Sanei, H., 2025. Maceral point counting for dispersed organic matter (DOM). Int. J. Coal Geol. 307, 104818.
Zimmerman, A.R., 2010. Abiotic and microbial oxidation of laboratory-produced black carbon (biochar). Environ. Sci. Technol. 44, 1295–1301.
Zimmerman, A.R., Gao, B., 2013. The stability of biochar in the environment. Biochar Soil Biota. 1, 240.